THE HOT INTERSTELLAR MEDIUM IN NGC 1399

Michael Loewenstein, Peter J. Serlemitsos, and the *BBXRT* Science Team
NASA-GSFC/USRA

1. INTRODUCTION

The first two high signal-to-noise, broad bandpass x-ray spectra of elliptical galaxies were obtained with the *Broad Band X-ray Telescope* (*BBXRT*) as part of the December 1990 Astro mission. These observations provided unprecedented information on the thermal and metallicity structure of the hot interstellar media in two ellipticals: NGC 1399, the central galaxy in the Fornax cluster, and NGC 4472, the brightest galaxy in the Virgo cluster. Here I report on the finalized analysis and interpretation of the $\sim$ 4000 sec of *BBXRT* data on NGC 1399.

2. SPECTRA

The orientation of the five *BBXRT* pixels superposed on the *Einstein* Observatory IPC image is shown in Figure 1. The central pixel covers the inner $2'$ of NGC 1399 and the outer pixels extend from $3.5' - 8.6'$, allowing us to detect any strong spatial gradients in temperature, absorption, or abundances. The spectra in the central and in one of the outer pixels are shown in Figures 2 and 3, respectively. The best fitting thermal spectra obtained using all of our available data have the following characteristics (with 90% confidence levels in parentheses). For the central pixel, $kT = 1.07(1.03 - 1.11)$ keV, $N_H = 9.8(4.2 - 16.)\ 10^{20}$ cm^{-2}, $Z = 0.75(0.51 - 1.1)$ solar; for the outer pixels, $kT = 1.11(1.08 - 1.19)$ keV, $N_H = 5.7(.063 - 10.)\ 10^{20}$ cm^{-2}, $Z = 0.30(0.24 - 0.38)$ solar. Note that the temperature gradient is small or non-existent, but a clear negative abundance gradient is indicated as can be seen by the relative emission line strengths in the spectra shown in Figures 2 and 3. There is marginal evidence (at the 3 σ level) for an Fe K line in the central pixel that must come from a seperate emitting component of higher abundance and/or temperature.

3. IMPLICATIONS

a) temperatures and dark matter

Previous efforts to infer the total gravitating mass in elliptical galaxies have been significantly impeded by an absence of accurate gas temperature measurements. The *BBXRT* spectrum of NGC 1399 provides a temperature determination of sufficient accuracy – the uncertainties in temperature are more than an order of magnitude less than for the only previously published x-ray (*Einstein* IPC) spectrum of NGC 1399 – to enable secure constraints on the dark matter content in an elliptical galaxy to be placed for the first time.

The solid curve in Figure 4 shows the mass-to-light ratio, (M/L_B) in solar units divided by h, *vs.* radius in arcseconds ($1'' \approx 65h^{-1}$ pc) for NGC 1399. This is derived from the equation of hydrostatic equilibrium, where we have used the analytic fit of Killeen & Bicknell to the x-ray surface brightness profile to derive the gas density profile, and the *BBXRT*-derived temperature of 1.1 keV. We have assumed that the gas is isothermal, as indicated by the consistency in the inner and outer pixel best-fit temperatures. While the derived value of $(M/L_B)h^{-1}$ inside $\sim 30''$ is probably not reliable due to possible departures from hydrostatic equilibrium and isothermality in a cooling flow, the total M/L_B within the *BBXRT* field of view is well-determined. The mass density of the non-luminous component evidently $\propto r^{-2}$ from $r < 100''$ to $r > 500''$, and dominates the potential for $r > 200 - 300''$. The integrated dark-to-luminous mass ratio inside the *BBXRT* aperture lies in the range 1.8 - 3.3, with the uncertainty due to the uncertainty in the stellar mass-to-light ratio. This ratio will, of course, continue to rise with radius until the halo density distribution steepens or truncates. The dashed extension to the curve in Figure 4 shows the mass-to-light profile extrapolated to the maximum radius where x-rays were detected above background by the IPC, assuming that the temperature remains constant at 1.1 keV.

We have also constructed stellar dynamical models of NGC 1399 to investigate whether the observed projected velocity dispersion profile is consistent with the x-ray derived mass profile. We have solved the equations of stellar dynamics, considering a wide range of velocity dispersion anisotropy distributions, to derive velocity dispersion profiles for stars orbiting in the potential determined by the x-ray emitting gas. The solid curve in Figure 5 shows one particular well-fitting model as well as the observed velocity dispersions on the western side of NGC 1399 from Bicknell *et al.* 1989. The solid curve in Figure 5 shows a well-fitting model for an assumed constant M/L_B of $14h$ that also provides a good fit to the optical data. The two model curves start to diverge significantly at about the edge of the observed spectroscopy; based on the

x-ray derived dark matter distribution we would expect the velocity dispersion profile to remain flat as the optical observations are extended to greater radii.

b) absorption by cold gas

The hydrogen column density in the central pixel derived from spectral fitting is $\sim 3 - 15\ 10^{20}$ cm^{-2} above the Galactic value. This corresponds to $\sim 10^9 M_\odot$ of cold gas, comparable both to the total mass lost by stars in the inner 10 kpc of NGC 1399 over the past 10^9 yr, and also to the total amount of hot x-ray emitting gas in that region. This significant amount of cold gas may be analagous to the large quantities of optically thick cloudlets responsible for x-ray absorption in some intracluster media, and is strong evidence that the central ISM in NGC 1399 is best described as a multi-phase medium. The outer pixel spectra suffer from significantly higher uncertainties at low energies – the hydrogen column density could be comparable to that seen in the central pixel, but is also consistent with the Galactic value.

c) abundances

The iron abundance, relative to solar, in the hot gas derived from the *BBXRT* central pixel x-ray spectrum of NGC 1399 is $Z_{Fe} = 0.51 - 1.1$, while the iron abundance derived from the combined *BBXRT* outer pixels spectra is significantly lower, $Z_{Fe} = 0.24 - 0.38$. This is a reflection of an abundance gradient in the galactic distribution of mass-losing stars, *i. e.* in the galaxy itself during the period when these old stars formed. This is the first evidence that the abundance gradients inferred from optical line-strength measurements persist well beyond the half-light radius.

The central pixel iron abundance is in excellent agreement with the iron abundance of the stars in a similar field inferred from multicolor optical photometry. This places a severe constraint on the Type Ia supernova (SNIa) rate in NGC 1399 since the injection of SNIa debris into the hot gas provides $\sim 0.6 M_\odot$ of iron for every SNIa. In fact, adopting the most conservative SNIa parameters, the limits on the SNIa Fe contamination inferred from the *BBXRT* spectra imply a specific SNIa rate $< 0.88h^2$ SNIa per 1000 yr per $10^{10}\ L_\odot$. This rate is ten times less than the value usually assumed based on a handful of observed SNIa events, and implies that SNIa are energetically and dynamically unimportant for the evolution of the hot ISM in NGC 1399. Therefore, a mostly subsonic cooling inflow is likely to be the most appropriate description of the dynamical state of the hot gas.

4. CONCLUSIONS

Because, as in spiral galaxies, the mass, energy, and metals in elliptical galaxy interstellar media originate in stars and supernovae, X-ray spectra of these galaxies are reflections of their structure and even of their evolution. Stellar orbits and abundances, the distribution of dark and luminous matter, and the evolution of supernova-progenitor binary stars all play strong roles in determining the characteristics of the X-ray emission. A $\sim$ 1 hr observation of NGC 1399 with the *Broad Band X-ray Telescope* has provided us with unique data on temperatures and abundances in the hot interstellar medium in an elliptical galaxy. With this data, we have inferred the presence of significant intrinsic absorption by cold gas, placed powerful and surprisingly small upper limits on the supernvova rate, and derived the distribution of the significant amount of dark matter present in NGC 1399.

Figure 1.

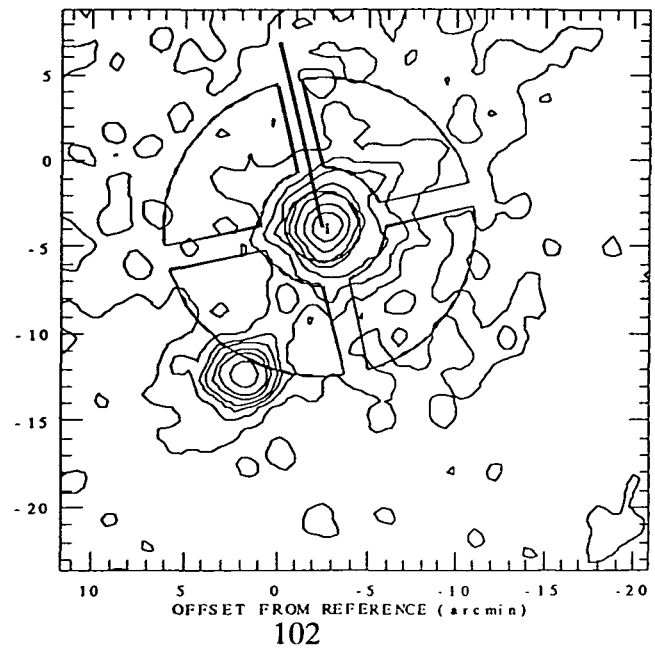

Figure 2.

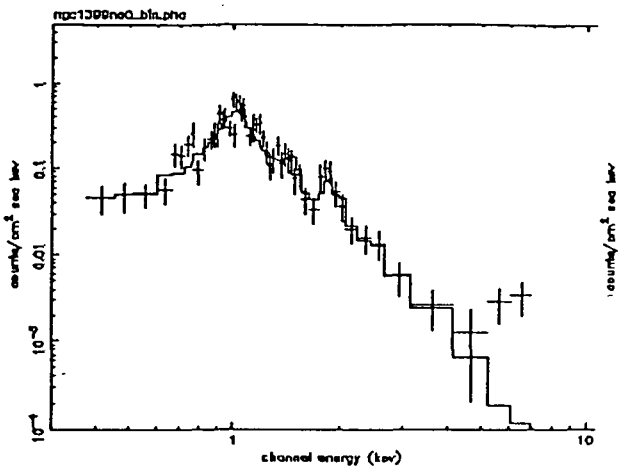

Night data from a0 det (2794 s)
fitted kT range 1.01-1.11 keV
fitted nH range 0.042-0.191 x 10^{22}

Figure 3.

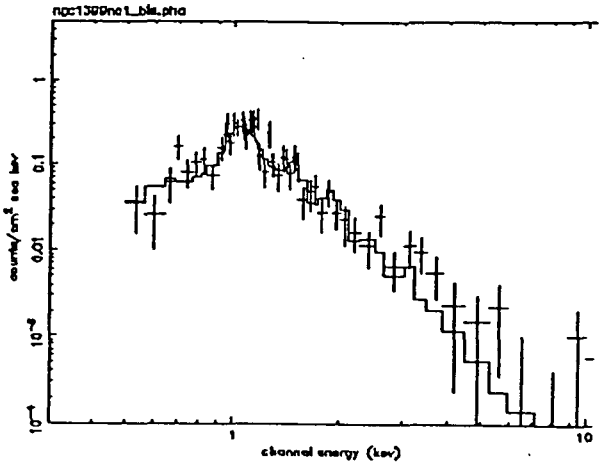

Night data from a1 det (2794 s)
fitted kT range 1.11 1.36 keV

Figure 4.

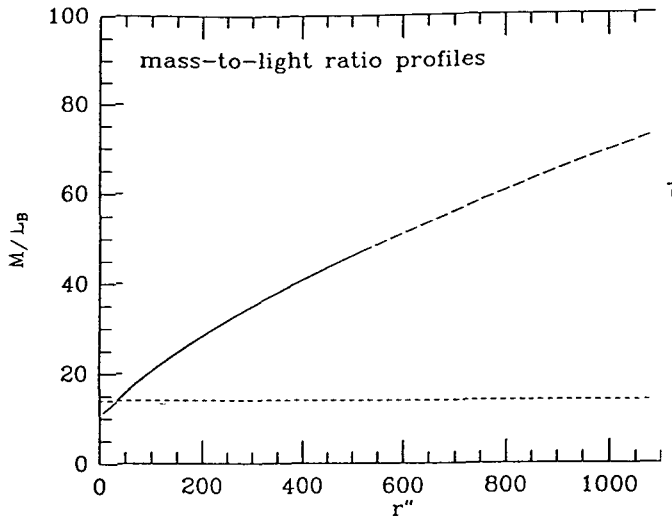

Figure 5.